**Forschungszentrum Karlsruhe**
Technik und Umwelt

**Wissenschaftliche Berichte**
FZKA 5713

# Dimensional Analysis and Scenario Discussion for the Spreading of a Corium Melt (EPR)

**P. Ehrhard**

**Institut für Angewandte Thermo- und Fluiddynamik**
**Projekt Nukleare Sicherheitsforschung**

**Mai 1996**

FORSCHUNGSZENTRUM KARLSRUHE
Technik und Umwelt
**Wissenschaftliche Berichte**
FZKA 5713

# Dimensional analysis and scenario discussion for the spreading of a corium melt (EPR)

**P. Ehrhard**
Institut für Angewandte Thermo- und Fluiddynamik
Projekt Nukleare Sicherheitsforschung

Forschungszentrum Karlsruhe GmbH, Karlsruhe
1996

Forschungszentrum Karlsruhe GmbH
Postfach 3640, 76021 Karlsruhe

ISSN 0947-8620

Abstract

Future generations of pressurized water reactors (e.g. the European Pressurized Water Reactor EPR) will have to realize safety concepts, which go significantly beyond the present standard. With respect to a severe core melt down accident, precautions need to be taken to ensure coolability of the corium melt and the integrity of the containment under all circumstances. In detail a reference concept relies on (a) accumulation of the melt below the pressure vessel, (b) dry spreading and stabilization of the melt on a horizontal spreading area of sufficient extent, (c) passively initiated flooding of the spreaded melt from above using water, (d) removing the decay heat by means of natural circulation within the pool and to the outside by immersed coolers connected to external heat exchangers.

The spreading of the corium melt on the spreading area represents one of the crucial questions as it determines the outcome of the scenario: If the melt spreads far enough, the thickness of the melt layer will be sufficiently small to ensure its coolability. On the other hand, if solidification within the melt restricts spreading, we are left with a large thickness of the melt layer. Thus, complete decay heat removal through the upper melt surface will not be possible leading eventually to a heat up of the melt and subsequently to erosion of the basemat material. Solidification may occur since the melt is strongly cooled from above by radiation and from below by some conduction within the basemat material.

From the above concept we conclude that spreading in presence of major solidified portions is the most critical configuration, leading eventually to a stop of the spreading flow. This problem is the focus of several investigations at the Forschungszentrum Karlsruhe

(FzK). In the framework of the large-scale KATS experiments the spreading of both metallic and oxidic components of a Thermite melt in ceramic-coated channnels is investigated. In parallel, physical models are being developed to describe the flow, heat transport and solidification processes during the spreading. Hereby additional small-scale experiments using low-melting waxes and alloys are performed to identify the basic physical phenomena. The present paper focuses on the development of models for the spreading flow. A dimensional analysis in conjunction with a scenario discussion is given.

Zusammenfassung

Ähnlichkeitsanalyse und Diskussion möglicher Szenarien
zur Ausbreitung einer Corium Schmelze

Zukünftige Druckwasserreaktoren wie der EPR werden bezüglich der Sicherheitskonzepte wesentlich weiter gehen als der derzeitige Standard. So müssen im Falle eines schweren Kernschmelzunfalls Maßnahmen getroffen werden, welche die Kühlbarkeit der Schmelze und die Integrität des Containments unter allen Umständen sicherstellen. Im einzelnen ist vorgesehen, (a) die Schmelze unter dem Druckbehälter aufzufangen, (b) die Schmelze danach auf einer ausreichenden Fläche trocken auszubreiten, (c) die ausgebreitete Schmelze passiv initiiert mit Wasser zu fluten und (d) die Nachzerfallswärme durch Zirkulation an sekundäre Wärmetauscher abzuführen.

Die Ausbreitung der Schmelze spielt hierbei eine Schlüsselrolle, da dieser Ablauf die Kühlbarkeit festlegt: Breitet sich die Schmelze vollständig aus, so wird die Schichthöhe genügend klein, um die Kühlbarkeit zu garantieren. Andererseits kann eine durch Erstarrung bedingte, unvollständige Ausbreitung zu großen Schichtdicken führen. Dann ist die vollständige Abfuhr der Nachzerfallswärme über die Oberfläche nicht sichergestellt und eine Aufheizung der Schmelze wird möglich. Dies bedingt die Gefahr einer Erosion der Bodenplatte. Erstarrung während der Ausbreitung kann auftreten, weil durch Strahlung eine effektive Kühlung der Schmelze von oben zu erwarten ist.

Aus dem oben Gesagten kann gefolgert werden, daß die Ausbreitung in Anwesenheit größerer erstarrender Anteile die

kritischste Konfiguration darstellt, welche unter Umständen die Ausbreitung gänzlich verhindern kann. Das Problem der Schmelzausbreitung wird derzeit an verschiedenen Stellen im Forschungszentrum Karlsruhe (FzK) untersucht. Mit den großskaligen KATS-Experimente wird die Ausbreitung beider Komponenten einer Thermitschmelze in Keramikkanälen betrachtet. Parallel hierzu werden physikalische Modelle entwickelt, welche die Strömung, den Wärmetransport und die Erstarrung in einer solchen Ausbreitungsströmung beschreiben. Hierzu werden auch kleinskalige Experimente durchgeführt, welche in Wachs und Woodsmetall die grundlegenden Phänomene studieren. Der hier vorliegende Bericht beschäftigt sich mit der Modellentwicklung für Ausbreitungsströmungen, indem auf der Basis von Ähnlichkeitsüberlegungen die möglichen Szenarien diskutiert werden.

Content

Nomenclature

| | |
|---|---|
| $Bi$ | *Biot* number, |
| $Ca$ | capillary number, |
| $c_p$ | specific heat of melt, |
| $Fr$ | *Froude* number, |
| $g$ | gravitational acceleration, |
| $H_0$ | vertical extend of spreading layer, |
| $H(t)$ | melt height in pool, |
| $H(X,\tau)$ | solution for the liquid/gas interface, |
| $\tilde{H}(\eta)$ | shape function, |
| $L_0$ | horizontal extend of spreading layer, |
| $p$ | pressure in melt, |
| $P$ | dimensionless pressure in melt, |
| $Pe$ | *Peclet* number, |
| $Pr$ | *Prandtl* number, |
| $q$ | strength of volume source, |
| $\dot{q}$ | internal heat sources in melt, |
| $Q$ | dimensionless heat sources, |
| $Re$ | *Reynolds* number, |
| $t$ | time, |
| $T_0, \nu_0, \kappa$ | initial temperature, kinematic viscosity and thermal conductivity of melt, |
| $T_\infty$ | ambient temperature, |
| $T$ | temperature in melt, |
| $T_s$ | solidification temperature, |
| $\bar{T}$ | average interface temperature, |
| $u_0$ | inflow velocity (at the gate), |

$u$, $w$ velocity components in melt,

$U$, $W$ dimensionless velocities,

$x$, $z$ spatial coordinates,

$X$, $Z$ dimensionless coordinates,

$\epsilon$ aspect ratio,

$\alpha$ exponent of time-law of volume,

$\tilde{\epsilon}$ emmisivity of interface,

$\mu$ local dynamic viscosity of melt,

$\lambda$ heat conductivity of melt,

$\eta$ similarity variable,

$\rho$ density of melt,

$\sigma$ surface tension,

$\tilde{\sigma}$ *Stefan-Boltzmann* constant,

$\tau$ dimensionless time,

$\theta$ dimensionless melt temperature,

$\theta$ dimensionless solidification temperature.

## 1. Introduction

To ensure the coolability of molten core debris as a consequence of a severe accident in a future European Pressurized Water Reactor (EPR), a core catcher design has been developed which relies on dry spreading of the core melt as the basis for a further cooling of the solidified layer. The spreading area is given as a solid concrete plate covered by ceramic tiles, preventing as much as possible an interaction of melt and structure material. The design concept is aimed at controlling the melt spreading in two steps. Firstly, after a large-area failure of the reactor pressure vessel the core debris are collected in a storage compartment below the pressure vessel (cf. I in figure 1). Due to internal heat sources the melt will be heated up and a homogeneous melt pool is expected to form. Secondly, the interaction of the hot melt with a properly designed gate leads to a gate failure at a defined temperature (II), thus initiating the release of the melt into the spreading compartment.As illustrated in figure 1, the gate is positioned between the melt storage compartment and the melt spreading area. It is pointed out here, that the controlled interaction of the melt with the gate material and the "defined" opening of the gate at a certain temperature level are of crucial importance and particular investigations on this problem are to be performed which are not the subject of this paper. During the first period there might be likewise interactions of the hot melt with the structure material of the storage compartment. These interactions can be minimized by covering the concrete adequately with refractory material. Once the gate opened,thirdly, a spreading of the melt occurs. Here three different regimes of melt spreading may be distiguished, depending on the

initial conditions in the melt (cf. III in figure 1): the inertial/gravitational regime, the viscous/gravitational regime and the crust controlled regime. These various types of spreading will be discussed below.

There are two other possibilities, which may change the above discussed scenario: a) If the reactor pressure vessel fails by a small break and at high temperatures, a hot melt jet will be ejected interacting with the structure material of the basemat structures (IV). This may lead to erosion and possibly to a failure of the structure if no sufficient protection by means of refractory ceramic material is provided. b) A small size leakage in conjunction with temperatures close to the solidus temperature may lead to a build-up of a debris pile consisting of solidified melt contacting the structure (V), preventing at least for some time the formation of a homogeneous melt pool as intended (I). This problem, however, might exist only for a certain period since internal heat sources will heat up the debris pile leading to a configuration similar to the case IIIc, the crust controlled regime.

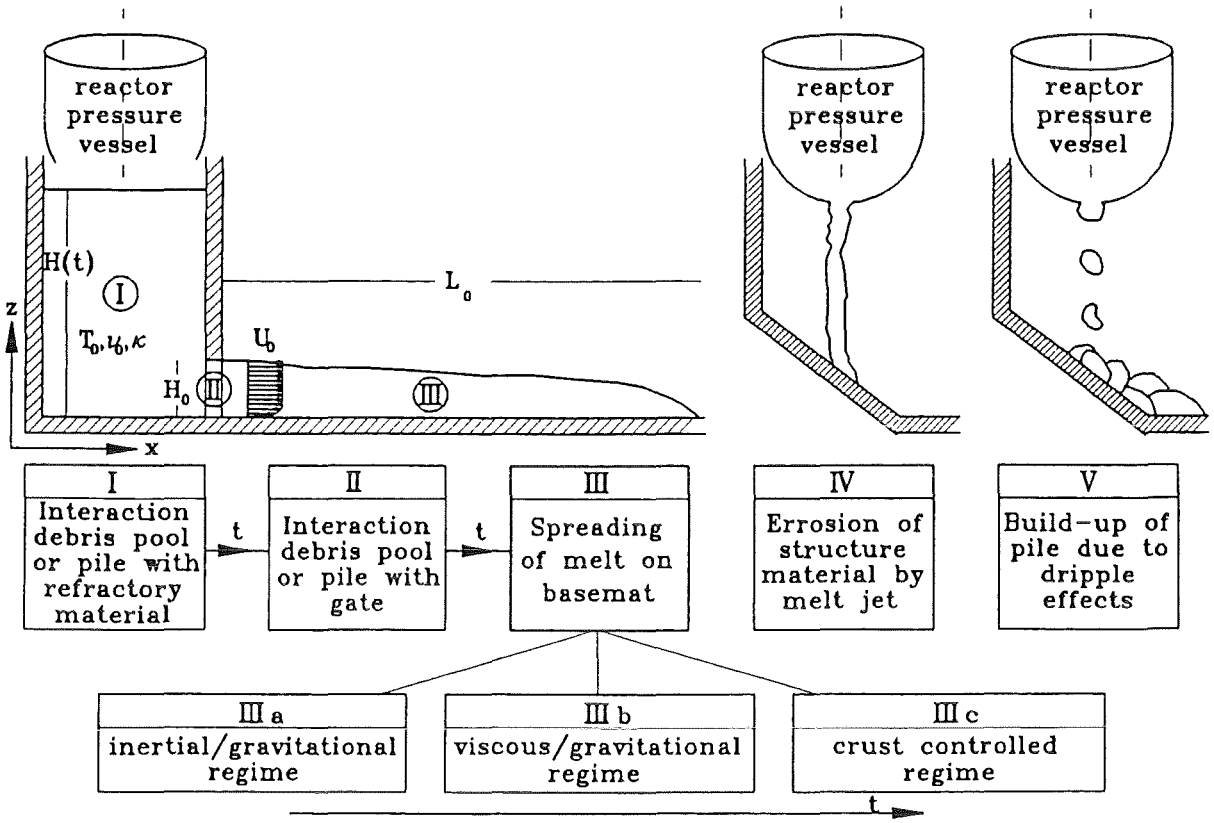


Figure 1: Possible configurations.

## 2. Dimensional Analysis

In the remainder of this paper we shall focus on the spreading of the melt on the horizontal plane (spreading area), as illustrated by III in figure 1. We shall neglect any interactions of the melt with the basemat material. Here three different regimes are possible, namely inertial/gravitational, viscous/gravitational or crust controlled spreading. To infer conditions for the various regimes it is helpful to first write down the basic equations and subsequently apply an appropriate scaling. From the dimensionless form further conclusions can be drawn with regard to the most important effects.

The basic equations for the plane problem $(x,z)$ are for mass conservation

$$u_x + w_z = 0, \tag{1}$$

for conservation of momentum, whereas a locally Newtonian liquid is considered if we assume $\mu = \mu(x,z)$,

$$\rho\left(u_t + uu_x + wu_z\right) = -p_x + \mu\left(u_{xx} + u_{zz}\right) + 2\mu_x u_x + \mu_z\left(u_z + w_x\right), \tag{2}$$

$$\rho\left(w_t + uw_x + ww_z\right) = -p_z + \mu\left(w_{xx} + w_{zz}\right) + 2\mu_z w_z + \mu_x\left(u_z + w_x\right) - \rho g, \tag{3}$$

and finally conservation of heat

$$\rho c_p\left(T_t + uT_x + wT_z\right) = \lambda\left(T_{xx} + T_{zz}\right) + \dot{q}. \tag{4}$$

These equations are generally valid in the liquid domain, limited by the solid basemat at $z = 0$ from below, the symmetry line at $x = 0$ from the left and by the melt/gas interface at $z = h(x,t)$ from above. On these boundaries the appropriate boundary conditions have to be formulated if a solution of the problem is sought. We continue, however, here by building up a scaling of the conservation equations. From geometry (cf. figure 1) it is immediately obvious that the

vertical length scale $H_0$ (gate height) is largely different from the horizontal length scale, which might be named $L_0$. Thus, at least for large times, we do have the small parameter $\epsilon = H_0/L_0 \ll 1$ involved. From that observation, we immediately infer the scales

$$
\begin{aligned}
X &= \frac{x}{L_0}, \qquad Z = \frac{z}{H_0}, \\
U &= \frac{u}{u_0}, \qquad W = \frac{w}{\epsilon u_0}, \\
\tau &= \frac{t}{L_0/u_0}, \qquad P = \frac{p}{\mu u_0 L_0/H_0^2}, \\
\Theta &= \frac{(T - T_\infty)}{(T_0 - T_\infty)} .
\end{aligned}
\tag{5}
$$

Besides the separate scales for $x,z$ we have defined a transport time scale, a viscous pressure scale and a standard temperature scale with $0 \le \Theta \le 1$. Implementing the above scales in the conservation equations *(1,2,3,4)* we get the dimensionless versions

$$U_x + W_z = 0, \tag{1a}$$

$$\epsilon Re\left(U_\tau + UU_x + WU_z\right) = -P_x + U_{zz} + \frac{\mu_z}{\mu} U_z + O(\epsilon^2), \tag{2a}$$

$$0 = -P_z - \frac{\epsilon Re}{Fr} + O(\epsilon^2) , \tag{3a}$$

$$\epsilon Pe\left(\Theta_\tau + U\Theta_x + W\Theta_z\right) = \Theta_{zz} + Q + O(\epsilon^2). \tag{4a}$$

Herein we have the dimensionless parameters *Reynolds* number, *Froude* number, *Peclet* number and the dimensionless internal heat source. The definitions are

$$
\begin{aligned}
Re &= \frac{u_0 H_0}{\nu} , \\
Fr &= \frac{u_0^2}{g H_0} , \\
Pe &= \frac{u_0 H_0}{\kappa} , \\
Q &= \frac{\dot{q} H_0^2}{\lambda (T_0 - T_\infty)} .
\end{aligned}
\tag{6}
$$

From the dimensionless set of conservation equations we can now draw conclusions with respect to the importance of various effects. We continue discussing the momentum equations *(2a)* and *(3a)*. Vertically a pressure term and a gravitational term arise (cf. equation *(3a)*). Horizontally an inertia term, a pressure term and two viscous terms are present. All of these effects might be important, depending on the actual magnitude of the parameters. Thus, a number of regimes arise which will now be discussed in detail.

## 2.1 Inertial/gravitational regime

Clearly, if

$$\epsilon Re \gg 1 \tag{7}$$

holds, the liquid motion is dominated by inertia effects (cf. equation *(2a)*). From the balance of inertia forces and pressure forces in *(2a)*, while viscous forces are neglected, it follows

$$P_x = O(\epsilon Re). \tag{8}$$

To maintain the balance between pressure forces and gravitational forces in equation *(3a)* we have to have

$$P_z = O(\epsilon Re), \tag{9}$$

$$\frac{\epsilon Re}{Fr} = O(\epsilon Re). \tag{10}$$

Formally, from $P = O(\epsilon Re)$ it can be concluded that the (viscous) pressure scale (cf. equation *(5)*) is not adequate for this inertial/gravitational regime. This is not surprising, as the scaling has been chosen for the viscous forces to be important. Nevertheless the conclusions *(8,9,10)* can be drawn and remain valid.

To summarize, the driving of the flow is provided by the gravitationally caused pressure distribution. From equation *(10)* an estimation for the outflow speed can be inferred, namely

$$u_0 \sim \sqrt{gH_0}\ . \tag{11}$$

One should be careful in interpreting equation *(11)*. $H_0$ is the constant gate height and $u_0$ is the outflow velocity, provided equation *(7)* holds. Thus, equation *(11)* gives the outflow velocity if there is no forcing by some other mechanism. In contrast, if the outflow is from a filled pool with liquid height $H(t)$ (cf. figure 1, I),

Bernoulli's equation might be applied to express the outflow velocity $u_0(t)$. This gives the forced outflow velocity

$$u_0(t) = \sqrt{2gH(t)}. \qquad (12)$$

In the inertial/gravitational regime the flow field will have a character as sketched in figure 2. We will have uniform velocity $u_0$ across most of the spreading layer of height $H_0$. In a very thin kinematic boundary layer at the solid wall (basemat) the velocity will drop from the bulk value $u_0$ to zero, regarding the no slip condition. Only in this thin boundary layer are viscous forces important. The thickness of this kinematic boundary layer can be estimated following e.g. *Schlichting (1982)* as

$$\frac{\delta}{H_0} \sim (Re)^{-1/2}. \qquad (13)$$

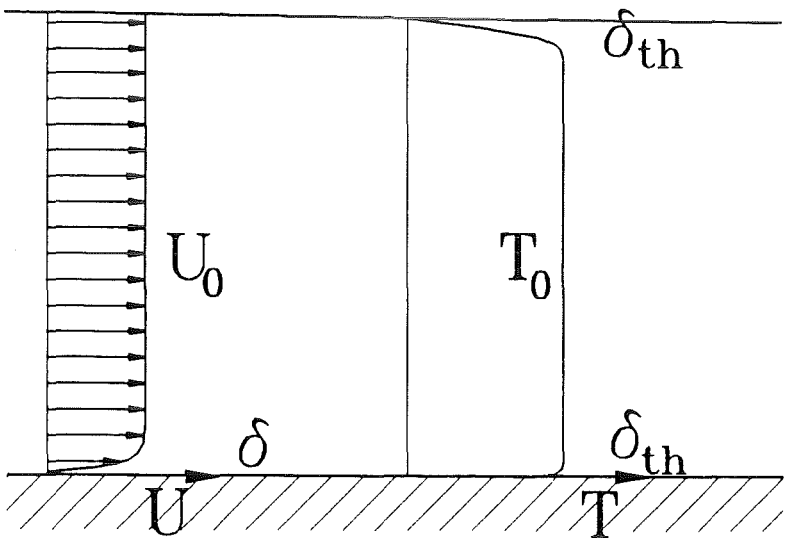


Figure 2: Situation in the inertial/gravitational regime.

Given this flow situation, the heat transport is now the focus. Since in equation *(4a)* the *Peclet* number occurs, we have to have

$$\epsilon Pe = \epsilon Re\ Pr \gg 1 \qquad (14)$$

to obtain a situation such that heat transport is mainly by convection. Formally, we then have an analogous form in equations *(2a)* and *(4a)*, i.e. transport of horizontal momentum and heat is analogous. In equation *(14)* the *Prandtl* number as ratio of kinematic and thermal diffusion coefficients depends only on the liquid. For oxidic melts, waxes or water $Pr \geq 1$ holds and therefore equation *(14)* is valid. A typical temperature profile for such a case is sketched in figure 2. Most of the spreading melt layer will be at temperature $T_0$ and only very thin thermal boundary layers at the liquid/solid interface and at the liquid/gas interface develop. Thus, only within those thin layers does conduction play a role, governing the heat fluxes downward into the horizontal plane and the radiative losses towards the ambient gas. Due to different heat fluxes, the upper and the lower thermal boundary layers are not equal in thickness. However, the order of magnitude of both layer thicknesses is comparable and can be estimated from *Schlichting (1982)* to be

$$\frac{\delta_{th}}{H_0} \sim (Pe)^{-1/2} . \qquad (15)$$

The thickness of the thermal boundary layers is already a good estimate for the thickness of possibly-forming crusts.

If we consider a metallic melt, featuring *Prandtl* numbers of $Pr \cong 10^{-2} \div 10^{-1}$, we have to be careful with respect to the validity of equation *(14)*. Since $\epsilon Re \gg 1$ is ensured within the inertial/gravitational regime, the product of $\epsilon Re$ and $Pr$ might yet be

finite. Thus, we would have to preserve both convective and conductive transport of heat in equation *(4a)*. That typically leads to thermal boundary layers, and therefore crusts, which are not thin.

The inertial/gravitational regime probably allows for a similarity solution of the pure hydrodynamic problem, i.e. of equations *(1a,2a,3a)* in the limit $\epsilon Re \gg 1$ (cf. *Hoult(1972)*).

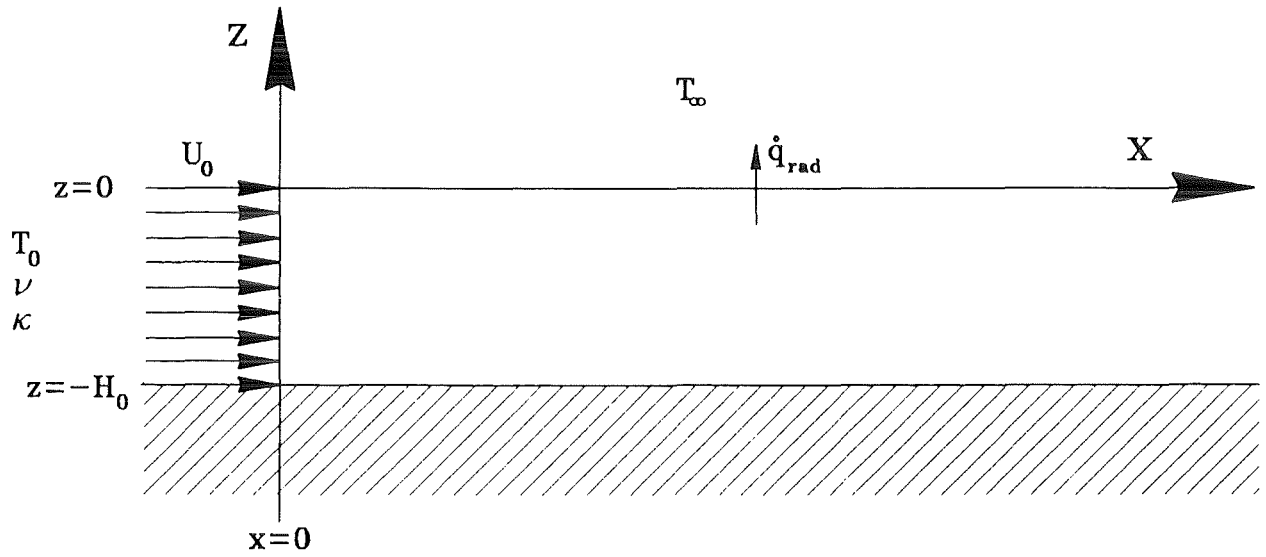


Figure 2a: Sketch of the problem.

Within the inertial/gravitational regime often so-called semi-infinite models can be applied. An example will be given here: We shall calculate the heat losses and the start of solidification for the case of a spreading high *Prandtl* number melt, cooled from above by radiation. As equation *(7)* always holds within the inertial/gravitational regime, large *Pr* numbers lead to

$$\epsilon\, Pe = \epsilon\, Pr\, Re \gg 1. \qquad (16)$$

The semi-infinite model, thus, is based on an extremely thin thermal boundary layer, whereas the flow in the spreading layer is considered to be "at infinity". Within this frame, the outer flow at some

distance from the liquid/gas interface can be considered as uniform in temperature and uniform and parallel in velocity. The flow vector is $\mathbf{v} = (u_0, 0)$ and temperature is $T_0$. Locally, the melt/gas interface is likewise parallel to the $x$-axis. Therefore, we have to solve mathematically the following problem: Equation *(4a)* reduces to the parabolic equation

$$\Theta_X = \frac{1}{\epsilon Pe}\,\Theta_{zz}, \tag{17}$$

which governs the heat transport. Hereby, the thermal boundary conditions (firstly in dimensional formulation)

$$\begin{aligned} &x=0: \quad T = T_0, \\ &z=0: \quad -\lambda \frac{\partial T}{\partial z} = h\,(T-T_\infty) = \tilde{\epsilon}\,\tilde{\sigma}\,(\bar{T}^2+T_\infty^2)(\bar{T}+T_\infty)\,(T-T_\infty). \end{aligned} \tag{18}$$

apply. These boundary conditions ensure a constant inlet temperature $T_0$ across the layer and give approximately the radiative heat losses at the melt/gas interface towards the ambient gas. Herein $\tilde{\epsilon}$ denotes the emmisivity, $\tilde{\sigma}$ the *Stefan-Boltzmann* constant and $\bar{T}$ is the average interface temperature, which might be estimated from the outlet and the solidification temperatures as $\bar{T} = (T_0+T_s)/2$.

We non-dimensionalize the above boundary conditions using the scales in equation *(5)* to obtain

$$\begin{aligned} &X=0: \quad \Theta = 1, \\ &Z=0: \quad \frac{\partial \Theta}{\partial Z} = -Bi\,\Theta. \end{aligned} \tag{19}$$

Herein the dimensionless parameter $Bi$ additionally appears. The definition is

$$Bi = \frac{H_0\,\tilde{\epsilon}\,\tilde{\sigma}\,(\bar{T}^2+T_\infty^2)\,(\bar{T}+T_\infty)}{\lambda}. \tag{20}$$

The *Biot* number quantifies the radiative heat transfer. The above dimensionless system of boundary conditions and differential equation has the solution (cf. *Carslaw & Jaeger 1959*)

$$\Theta = \mathrm{erf}\left\{\sqrt{\frac{Pe\epsilon Z^2}{4\,X}}\right\} + \exp\left\{Bi\;Z + \frac{Bi^2 X}{Pe\;\epsilon}\right\}\mathrm{erfc}\left\{\sqrt{\frac{Pe\epsilon Z^2}{4\,X}} + Bi\sqrt{\frac{X}{Pe\epsilon}}\right\}, \qquad (21)$$

and therefrom the temperature at the melt/gas interface is given by

$$\Theta(X,Z=0) = \exp\left\{\frac{Bi^2 X}{Pe\;\epsilon}\right\}\mathrm{erfc}\left\{Bi\sqrt{\frac{X}{Pe\epsilon}}\right\}. \qquad (22)$$

We shall expect solidification in principle as soon as temperature falls below the solidification temperature $T_s$. To form a crust of considerable thickness, however, a range of extent $c$ at the melt/gas interface needs to be below solidification temperature. Given the required crust thickness $c$, in dimensionless form $C = c/H_0$, the condition is

$$\Theta(X=L,Z=-C) \le \Theta_s = \frac{(T_s - T_\infty)}{(T_0 - T_\infty)}\,. \qquad (23)$$

The value of $L$, therefore, will depend on the parameters $Bi$, $Pe$ and $\Theta_s$. Moreover, a dependence on the required crust thickness $C$ follows. Finally, after solving the above problem it is important to ensure that the temperature disturbance due to cooling the melt/ambient interface has not penetrated towards the bottom of the melt. Therefore, $\Theta(X=L,Z=-1)$ should still be close to unity. In other words, it needs to be ensured that the semi-infinite approach holds.

We now apply the above semi-infinite model to a situation related to the KATS experiments. Provided a constant flow rate in time is present at the gate, the formation of a solid crust on top of the spreading oxidic part of the thermite melt is estimated. Table I gives

the properties, initial data and geometric data:

| | | | |
|---|---|---|---|
| heat conductivity $Al_2O_3$ | $\lambda$ | $1.7$ | $W/(mK)$ |
| specific heat $Al_2O_3$ | $c_p$ | $1.65\ 10^3$ | $Ws/(kgK)$ |
| density $Al_2O_3$ | $\rho$ | $2.8\ 10^3$ | $kg/m^3$ |
| viscosity $Al_2O_3$ | $\mu_0$ | $4.1\ 10^{-2}$ | $Ns/m^2$ |
| solidification temperature | $T_s$ | $2054$ | $°C$ |
| initial temperature | $T_0$ | $2150$ | $°C$ |
| initial velocity | $u_0$ | $2.73$ | $m/s$ |
| gate height | $H_0$ | $0.05$ | $m$ |
| emmisivity | $\tilde{\epsilon}$ | $0.8$ | $1$ |
| *Stefan-Boltzmann* constant | $\tilde{\sigma}$ | $5.7\ 10^{-8}$ | $W/(m^2K^4)$ |

Table 1: Properties in the KATS experiments (oxidic melt).

Therefrom the dimensionless groups, relevant to the oxidic melt in the KATS experiments, can be calculated. We get

$Re = 9322,$

$Pe = 370950,$

$Bi = 20.49,$

$\Theta_s = 0.9549,$

$(Pr = Pe/Re = 39.8).$

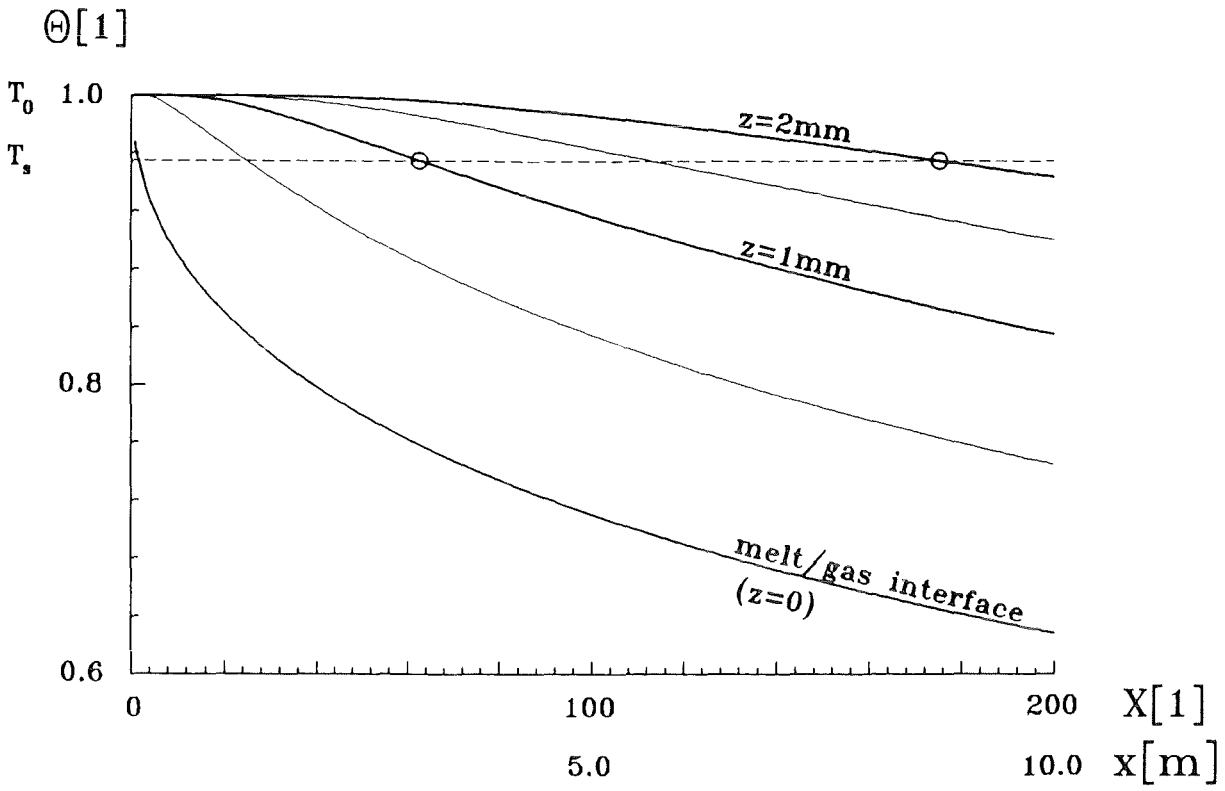


Figure 2b: Temperature profiles along the spreading direction in various depths.

Using this set of parameters, we solve for the temperature field and the results are plotted in figures 2b, 2c and 2d. Figure 2b shows temperature profiles as function of $X$ for varied values of $Z$. We recognize at the outlet ($X = 0$) all temperatures at $\Theta = 1$. The temperature at the melt/gas interface very soon falls below the solidification temperature (dashed line). To evaluate the formation of a crust, we have to focus on the temperature profiles in some depth beneath the melt/gas interface. The profile *2 mm* (*1 mm*) below the melt/gas interface shows temperature falling below solidification temperature at a distance of $L_2 \cong 8.7\ m$ ($L_1 \cong 3.1\ m$). That means, a crust of *2 mm* to be formed needs a channel length of *8.7 m* ! In other words, a considerable effect of a crust onto the spreading seems

unlikely even for a channel length of a few ten meters.

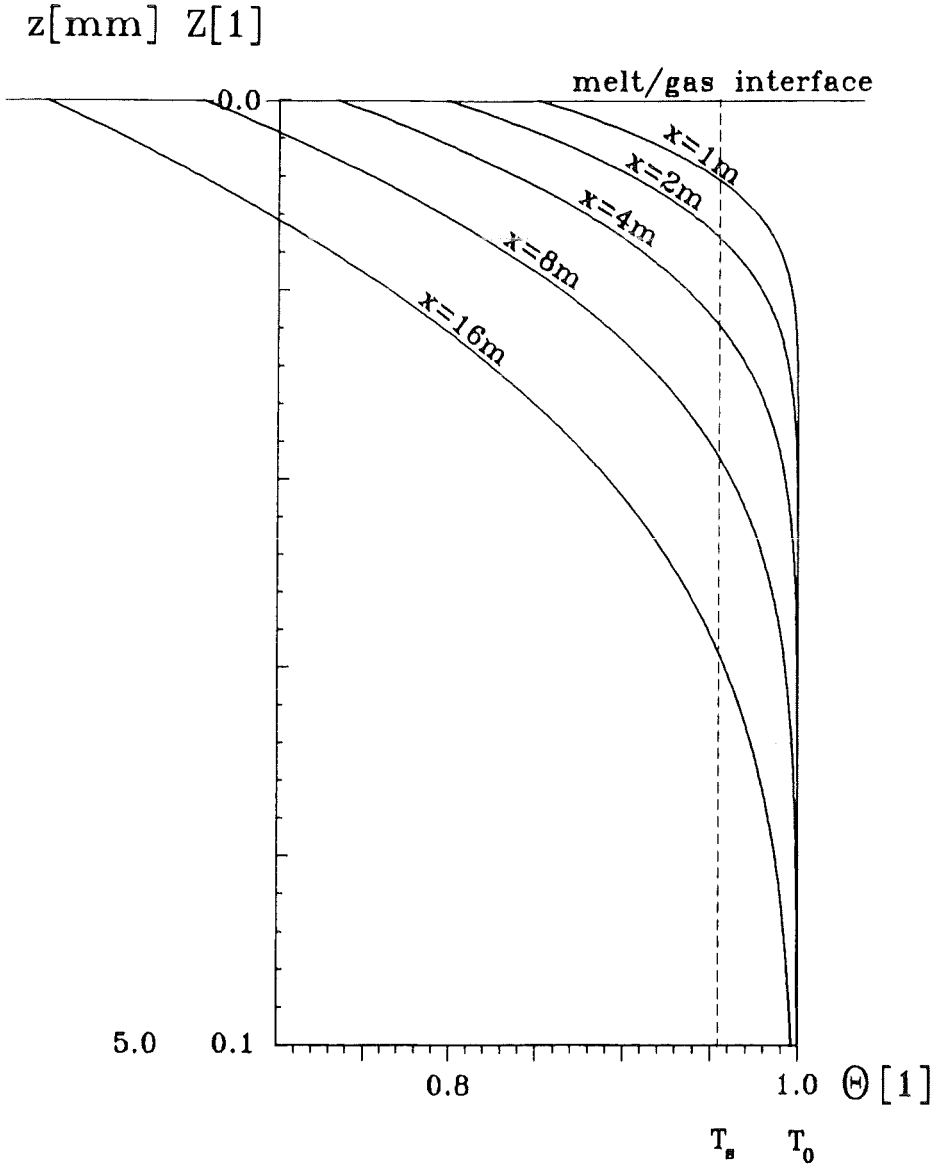


Figure 2c: Temperature profiles across the melt layer for various distances from the gate.

The check for consistency of the model is conducted in figure 2c. Here we plot temperature profiles of the melt as function of depth *Z*. We recognize pronounced thermal boundary layers at the melt/gas interface. Even in a distance of $x = 16\ m$ the thermal disturbance has only penetrated into *10 %* of the melt layer, while the rest of the

melt, adjacent to the wall, is not affected by the radiative cooling. Thus, the semi-infinite approach obviously holds.

The build up of the crust, thus, can be summarized using figure 2d. Here the portion of the melt, which is below solidification temperature, is hatched. Therefrom a solid layer of a thickness of about *1/4* of the liquid height $h_0$, i.e. *12.5 mm*, is obtained after a spreading length of *200 m*.

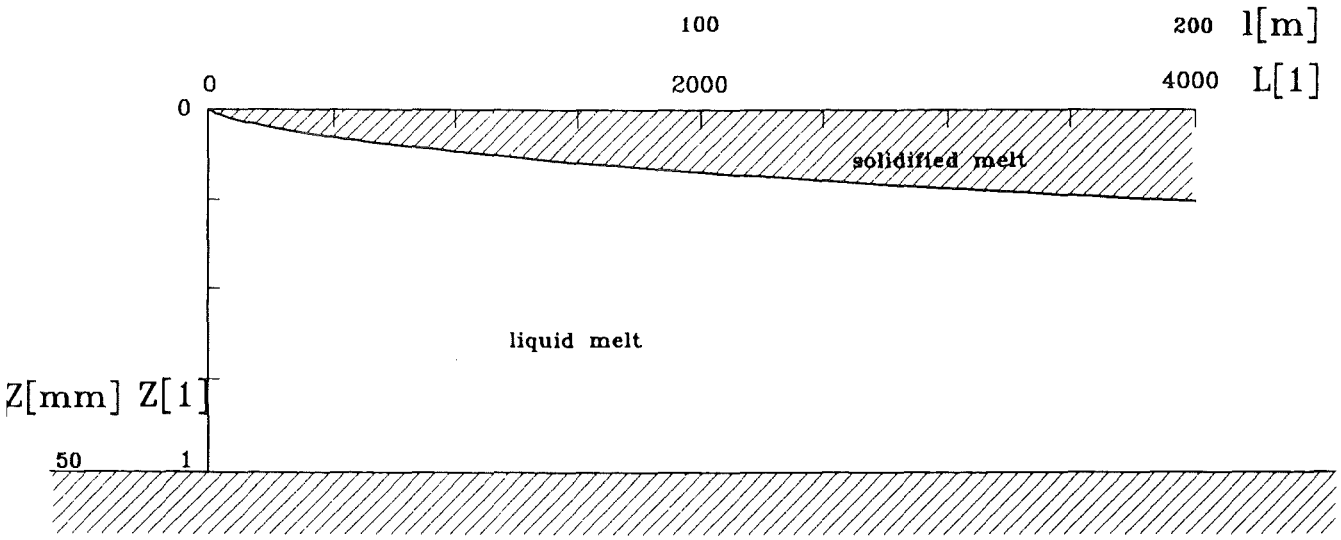


Figure 2d: Solidified portion of the layer.

## 2.2 Viscous/gravitational regime

A second limiting cases results if

$$\epsilon Re \ll 1 \tag{24}$$

holds. From equation *(2a)* a balance between viscous forces and pressure forces is obvious, whereas inertial forces are neglected. Equation *(3a)* again shows a vertical pressure gradient, governed by gravitational forces, driving the flow. Therefrom

$$\frac{\epsilon Re}{Fr} = O(1) \tag{25}$$

is readily inferred for this viscous/gravitational regime. Equation *(25)* allows likewise for an order of magnitude estimation of the outflow velocity, namely

$$u_0 \sim \frac{H_0^3 \, g}{L_0 \, \nu} \, . \tag{26}$$

If the outflow velocity is forced by some other means, e.g. if a filled pool is present with liquid height $H(t)$, equation *(12)* can be used to express $u_0(t)$ and in conjunction with equation *(26)*

$$L_0(t) \sim \frac{H_0^3}{\nu} \left\{ \frac{g}{2H(t)} \right\}^{1/2} , \tag{27}$$

an estimation of the spreading length, follows.

By carefully inspecting equation *(2a)* we realize that besides the usual dissipative viscous term due to the local viscosity $\mu$, a second term due to $\mu = \mu(X,Z)$ is present. The dimensionless parameter $\mu_Z/\mu$ characterizes this effect, whereas $\mu_Z$ is the vertical derivative of the local viscosity in the frame of the dimensionless variable $Z$ (cf. equation *(5)*). The dependancy $\mu(X,Z)$ has been allowed to include effects of solidification. During solidification the temperature field will strongly influence viscosity - at solidification temperature

leading even to an infinite viscosity. The attemp here is to treat solidified regions to some extent by applying a higher viscosity, or mathematically, to formulate some function $\mu = f(\Theta(X,Z))$. This, of course, provides only an approximative way of describing solidification, whereas e.g. the release of latent heat at the solidification front must be treated explicitly in a more rigorous model.

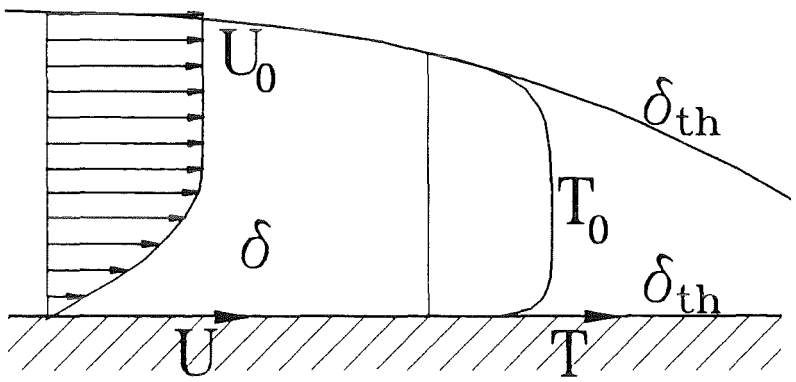


Figure 3: Situation in the viscous/gravitational regime.

In the viscous/gravitational regime the flow field will occur as sketched in figure 3. The kinematic boundary layer will extend across most of the spreading layer such that

$$\frac{\delta}{H_0} = O(1) \qquad (28)$$

holds. From the assumption *(24)* it is not yet clear what effects are relevant within the heat transport equation. A purely conductive heat transport across the layer results if

$$\epsilon Pe = \epsilon Re\ Pr \ll 1 \qquad (29)$$

is valid. That is the case for all liquids with small *Prandtl* numbers $Pr \leq 1$, e.g. for liquid metals. A typical temperature profile for such a situation is likewise given in figure 3. Relatively thick thermal boundary layers at both sides are characteristic for such a situation. Again both thermal boundary layers are different in thickness due to different heat fluxes at the bottom and at the interface. Analogous to the flow field we have an order of magnitude estimation for their thickness

$$\frac{\delta_{th}}{H_0} = O(1) \ . \qquad (30)$$

Thus, in this case relatively thick solid crusts, comparable to $\delta_{th}$ in thickness, may build up.

A different situation, however, occurs if large *Prandtl* number fluids as oxidic melts, oils or waxes are considered. In these cases equation *(29)* may be violated and the complete heat transport equation *(4a)*, including convective transport, needs to be used as the basis. Typically the thermal boundary layers in such a case would be rather thin.

With respect to the viscous/gravitational regime there is litte theoretical work in the literature. Huppert *(1982)* considered the pure hydrodynamic problem ($T, \mu = constant$). Thus, he solves the following set of equations

$$\begin{aligned} U_x + W_z &= 0, \\ 0 &= -P_x + U_{zz}, \\ 0 &= -P_z - \frac{\epsilon\ Re}{Fr}, \end{aligned} \qquad (31)$$

and applies the boundary conditions

$$\begin{aligned} &Z = 0\colon\ U = 0,\ W = 0, \\ &Z = H\colon\ W = UH_X + H_\tau, \\ &\qquad U_Z = 0 + O(\epsilon^2), \\ &\qquad \Delta P = 0 + O(\frac{\epsilon^3}{Ca}). \end{aligned} \tag{32}$$

These boundary conditions, thus, ensure within the current approximation no-slip at the solid/liquid interface and a tangential flow at the liquid/gas interface with vanishing shear stress. Moreover, due to $\epsilon^3/Ca \ll 1$, the pressure jump across the liquid/gas interface is negligible if the capillary number $Ca = \mu u_0/\sigma$ is not too small. The capillary number measures the ratio of gravitational and capillary forces. Integrating the vertical momentum equation in *(31)* we obtain firstly the pressure field

$$P(X,Z,\tau) = \frac{\epsilon\ Re}{Fr}\ (H-Z). \tag{33}$$

Using the horizontal momentum equation in *(31)* in conjunction with the boundary conditions *(32)* and the pressure *(33)*, the velocity field is readily inferred to be

$$U(X,Z,\tau) = \frac{\epsilon\ Re}{Fr}\ H_X(\ \frac{Z^2}{2} - HZ). \tag{34}$$

By integrating the continuity equation in *(31)* and using equations *(34)* and the tangential flow condition in *(32)* we finally arrive at the evolution equation for $H(X,\tau)$, i.e.

$$H_\tau - \frac{1}{3}\ \frac{\epsilon\ Re}{Fr}\ \left\{H^3 H_X\right\}_X = 0. \tag{35}$$

This partial differential equation *(35)* and volume condition within

the spreading layer, i.e.

$$\int_0^{A(\tau)} H(X,\tau)\, dX = V(\tau) = \frac{q\, L_0^{\alpha}}{u_0^{\alpha}\, H_0\, L_0}\, \tau^{\alpha} \tag{36}$$

are the complete formulation of the problem. The flow boundary conditions are already fullfilled. $A(\tau)$ herein denotes the position of the contact line. Following Huppert *(1982)* this set of equations *(35, 36)* allow for a similarity solution. Using the similarity transformations

$$\eta = \frac{X}{c_0\, \tau^{(3\alpha+1)/5}}, \qquad H(\eta,\tau) = \tilde{H}(\eta)\, c_1\, \tau^{(2\alpha-1)/5}, \tag{37}$$

we obtain an ordinary differential equation for the shape function $\tilde{H}(\eta)$, namely

$$\left(\tilde{H}^3 \tilde{H}_{\eta}\right)_{\eta} + \frac{3\alpha+1}{5}\, \eta\, \tilde{H}_{\eta} - \frac{2\alpha-1}{5}\, \tilde{H} = 0, \tag{38}$$

and the volume condition reduces to

$$\int_0^1 \tilde{H}\, d\eta = 1. \tag{39}$$

The constants within the similarity transformations *(37)* are given by

$$c_0 = \left\{\frac{\epsilon\, Re}{3\, Fr}\right\}^{1/5} \left\{\frac{q\, L_0^{\alpha}}{u_0^{\alpha}\, L_0\, H_0}\right\}^{3/5}, \qquad c_1 = \left\{\frac{3\, Fr}{\epsilon\, Re}\right\}^{1/5} \left\{\frac{q\, L_0^{\alpha}}{u_0^{\alpha}\, L_0\, H_0}\right\}^{2/5}. \tag{40}$$

The solution to the ordinary differential equation *(38)* and the integral condition *(39)* for general dependancies $V \sim \tau^{\alpha}$ need to be obtained by numerical integration (e.g. using Gears's method). In particular for constant volume, i.e. $\alpha = 0$, there exists an analytical

solution to the problem, namely

$$\tilde{H}(\eta) = \left(\frac{3}{10}\right)^{1/3}\left(1 - \eta^2\right)^{1/3} . \qquad (41)$$

Figure 3a presents two results, obtained from equations *(38)*, *(39)*, namely for constant volume ($\alpha=0$) and for a constant inflow ($\alpha=1$) across the left boundary at $X = 0$. Shown in both cases are the initial contours with identical volumes, obtained for $\tau = 1$. The second contours in both cases are obtained for $\tau = 3$ and show additionally streamlines and profiles of $U(Z)$. We recognize for the constant volume case a flow from the centre region of the liquid layer towards the propagating front. The velocity profile $U(Z)$, hereby, extends across the complete liquid layer and does not exhibit any boundary layer character. If we concentrate on the constant inflow case, the progression of the front is clearly faster, while again the profile $U(Z)$ extends across the whole layer. It should be pointed out here that the solution for the front profile and flow field in the immediate vincinity of the contact line $X = A(\tau)$ is incorrect due to several simplifying assumptions.

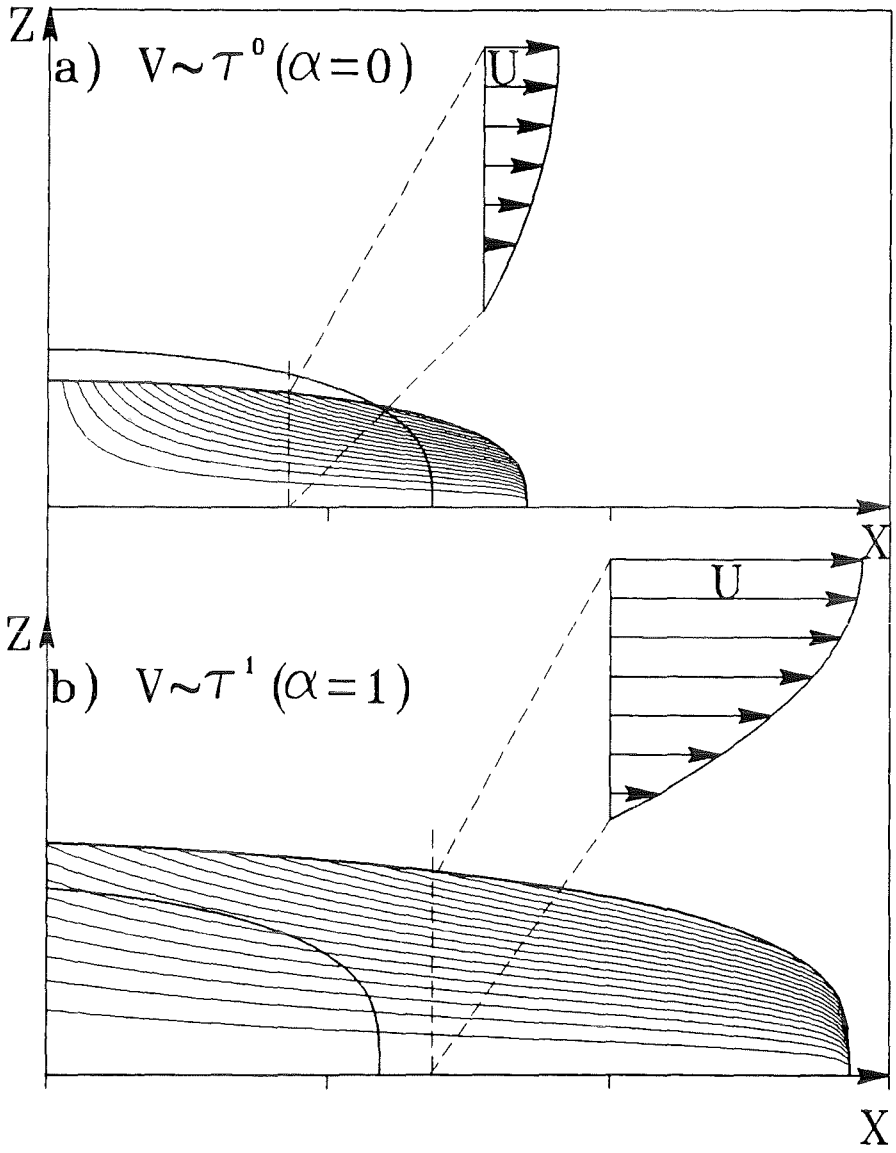


Figure 3a: Contours and streamlines for the the viscous/gravitational solution.

## 2.3 Crust controlled regime

There is very little work in the literature on a situation, where a crust has already formed leading to a stop of the spreading flow. The problem in a simple geometric configuration is sketched in figure 4. Given the initial solid contour $h_o(x,t)$, internal heat sources $\dot{q}(x,z,t)$ due to production of decay heat will heat up the crust, forming a liquid zone in the centre region described by $h_i(x,t)$. The dominant heat sink will be by radiation from the gas/solid interface into the ambient, whereas heat fluxes into the basemat or the adjacent layer material (hatched in fig. 4) will be of minor importance. Within the liquid zone natural convection will contribute substantially to the heat transport. Given sufficiently strong heat sources, the liquid zone will grow in time until either the crust opens at position 1 or the crust starts sliding at position 2 (cf. fig. 4). This would lead to a new start of the spreading flow. We should remark here, that the scaling as introduced in chapter 2 of this paper is not adequate for this problem. In particular the separate spatial scales are not present. Again, this problem is hardly understood and fundamental investigations are needed.

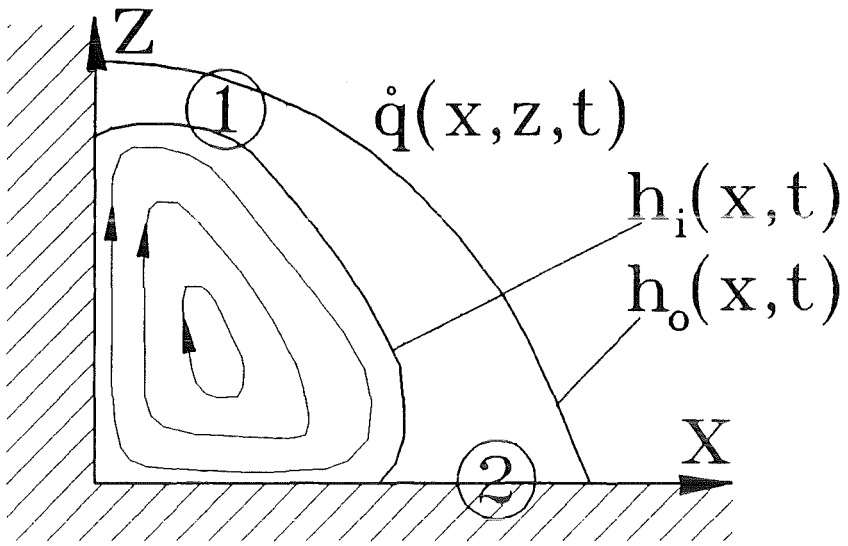


Figure 4: Situation in the crust controlled regime.

## 3. Summary

We have developed a scenario for melt propagation on a core melt retention device designed for a pressurized water reactor (e.g. EPR). In particular we have addressed aspects associated with the melt-through of the reactor pressure vessel and the subsequent events, leading to a coolable layer of solidified melt on the floor of the spreading compartment. The most critical questions of this sequence have been identified. These are:

1.) The interaction of a hot, high pressure melt jet with the structure or with the refractory material. This problem is not sufficiently understood, and must be investigated furtheron.

2.) The interaction of the melt with the gate, and the postulated "defined" opening is a crucial question. A design for the gate is being developed by the venders. The adequate functioning of this component under simulated accident conditions has to be thoroughly investigated.

3.) The question of melt spreading for given initial conditions and geometry another important issue. This problem is being investigated by several research groups, e.g. by CEA in Grenoble, by CEA in Cadarache, by Siemens in Erlangen and by the Forschungszentrum Karlsruhe. This problem has also been addressed in this article.

4.) The remelting of debris piles and the onset of melt efflux therefrom is a not well understood ingredient of the outlined melt spreading scenario. The physics behind this problem has to be investigated in more detail. We have started at the Forschungszentrum Karlsruhe to look into this problem both numerically (finite difference method) and experimentally (model melts in small scale).

We shall continue focusing on the spreading of melts. The dimensional analysis in this paper demonstrates that once the parameters outflow speed $u_0$, outflow height $H_0$ and the properties of the melt are known, via the dimensionless groups *Reynolds* number, *Froude* number and *Prandtl* number, the type of the spreading flow is readily determined.

The inertial/gravitational regime is not really a problem as it ensures undisturbed spreading, developing only thin kinematic boundary layers. For most melts thin thermal boundary layers, and therefore thin crusts, will develop.

Analyzing the viscous/gravitational regime, firstly viscous effects develop thick kinematic boundary layers, dissipating the kinetic energy of the spreading flow. Secondly, if viscosity is considered to strongly depend on temperature, a term due to $\mu(x,z)$ arises in the horizontal momentum equation, providing additional dissipation of considerable strength. Thirdly, for most melts the thermal boundary layers will likewise be thick and thus, the dissipation due to $\mu(x,z)$ is present in large portions of the flow field. The viscous/gravitational regime, even in the presence of strongly increasing viscosity due to solidification, is the most

critical case as it eventually stops the spreading flow. With respect to this problem, models from several places should be available shortly, in particular for modelling solidified regions.

The distinction between the various spreading regimes can be seen as a time dependent evolution. If initially due to large $(u_0 H_0)$ and small $\nu_0$ (large $T_0$) the spreading flow is inertia dominated, a development towards a viscosity dominated situation will follow. This change of spreading regime, as time progresses, is due to a decrease of $(u_0 H_0)$, an increase of $\nu_0$ as consequence of heat losses and a decrease of $\epsilon = H_0/L_0$. All of these changes will shift the dimensionless groups towards the viscous/gravitational regime. A further decrease of temperature with time finally will lead to solidification and thus, the crust controlled regime is entered.

## 4.References


D.P. Hoult 1972, Oil spreading on the sea, Ann. Rev. Fluid Mech. 4, 341ff.

H. Schlichting 1982, Grenzschicht-Theorie, Verlag G. Braun, Karlsruhe.

H. Huppert 1982, The propagation of two-dimensional and axisymmetric viscous gravity currents over a rigid surface, J. Fluid Mech. 121, 47ff.

H.S. Carlslaw & J.C. Jaeger 1959, Conduction of heat in solids, Claredon Press, Oxford.